

# Observation of coherent elastic neutrino-nucleus scattering

COHERENT Collaboration

2019/06/19

Jae Jin Choi

# Contents

---

- Observation of coherent elastic neutrino-nucleus scattering( $CE\nu NS$ )
- Neutrino Elastic-scattering Observation with NaI(NEON)

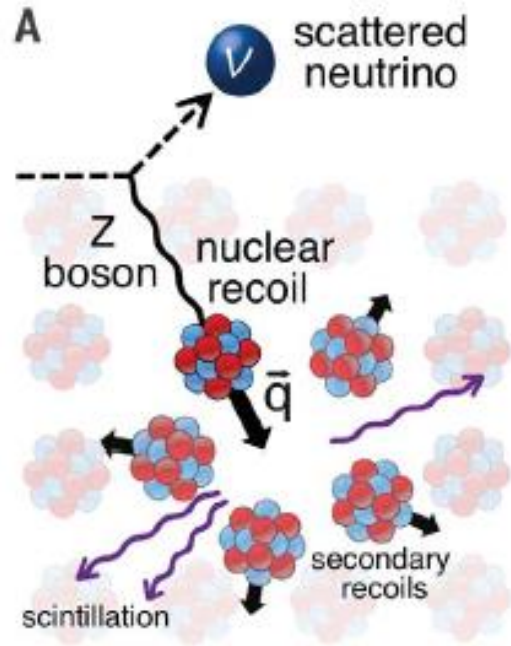
# Motivation

---

- To detect coherent neutrino-nucleus scattering(undetected forty years after its first description)
- To expand knowledge of neutrino properties(sterile neutrino, neutrino magnetic moment, nuclear structure and so on)
- To confirm limitation of WIMP-nucleus scattering cross section(background from solar and atmospheric neutrinos)

# Background(Neutrino interactions)

- Neutrino-nucleus scattering diagram



- Neutral-current neutrino scattering(Z boson)
- Neutrinos are capable of coupling to quarks through the exchange of neutral Z bosons
- Coherent interactions between neutrinos and all nucleons present in an atomic nucleus
- Scintillation from interactions can be detected

**Fig. 1. Neutrino interactions.** (A) Coherent elastic neutrino-nucleus scattering. For a sufficiently small momentum exchange ( $q$ ) during neutral-current neutrino scattering ( $qR < 1$ , where  $R$  is the nuclear radius in natural units), a long-wavelength Z boson can probe the entire nucleus and interact with it as a whole. An inconspicuous low-energy nuclear recoil is the only observable. However, the probability of neutrino interaction increases substantially with the square of the number of neutrons in the target nucleus. In scintillating materials, the ensuing dense cascade of secondary recoils dissipates a fraction of its energy as detectable light. (B) Total cross sections from CEvNS and some known neutrino couplings. Included

# Why CsI[Na] scintillator?

- CsI[Na] detector

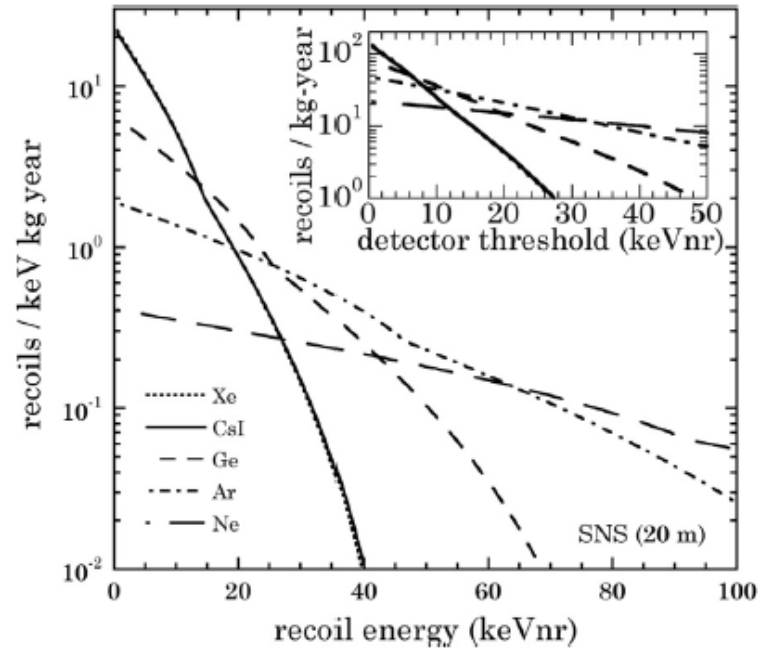


Fig. 1. Comparison between nuclear recoil energy spectra from different CENNS detector materials at the SNS. The calculation follows the formalism of [2] and includes a nuclear form factor as in [20]. Approximately  $0.13 \nu$  are produced per proton on target, per flavor. For present SNS running conditions, the neutrino flux at 20 m from the SNS interaction point is  $\sim 1.7 \times 10^7 \text{ cm}^{-2} \text{ s}^{-1}$ , per flavor. *Inset:* CENNS interaction rate integrated above detector threshold. The tradeoff between coherent enhancement to the cross-section and recoil energy is evident in this figure: heavy targets are favored, but only as long as a sufficiently low threshold can be achieved.

Calculation using formalism

- **High mass** of both recoiling species (Cs:133, I:127)
  - > large coherent enhancement to the CE $\nu$ NS cross-section (approximately scaling with the square of the number of neutrons in the nucleus)
- Tradeoff between coherent enhancement to the cross-section and recoil energy
  - > consider low recoil energy and achieve low threshold in this experiment

# Why CsI[Na] scintillator?

- CsI[Na] detector

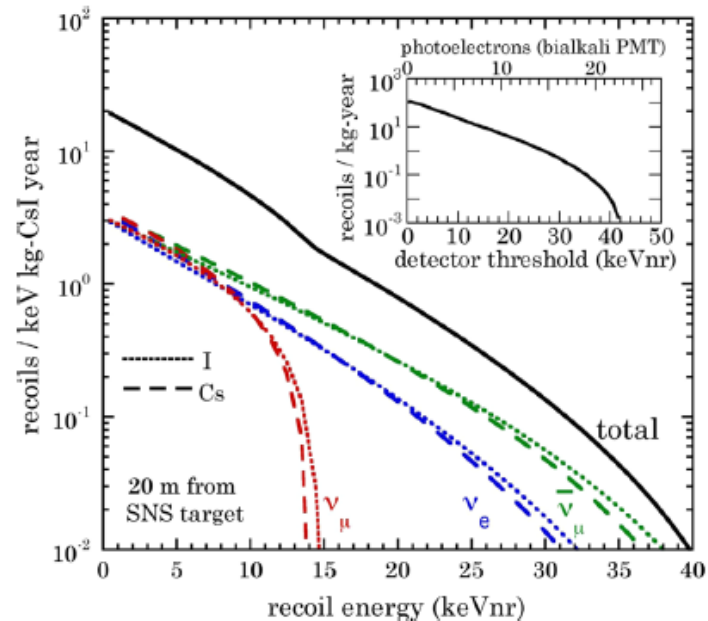


Fig. 2. Response of CsI[Na] to CENNS at the SNS, segregated by recoiling species and neutrino flavor. The sodium dopant is present with a fractional mass of just  $10^{-4}$ – $10^{-5}$ , playing no significant role as a target. Cs and I respond almost identically to a given neutrino flavor, simplifying the task of understanding the detector response. *Inset:* Integrated rate above detector threshold in nuclear recoil energy (keVnr). This energy scale is translated into number of detected photoelectrons (PEs) in a conventional bialkali PMT through the quenching factor measured in Section 3 and the light yield in the 2 kg prototype at few keVee (Section 4). Test runs performed in similar conditions to those expected at the SNS show that a threshold of 4 PE ( $\sim 7$  keVnr) is reachable with sufficient signal-to-background ratio (Section 5).

- Both recoiling species are essentially indistinguishable due to their similar mass  
-> Simplifying the understanding of the response of the detector

2015 R&D paper

# Why CsI[Na] scintillator?

- Afterglow(phosphorescence) in CsI[Na] and CsI[Tl] scintillators

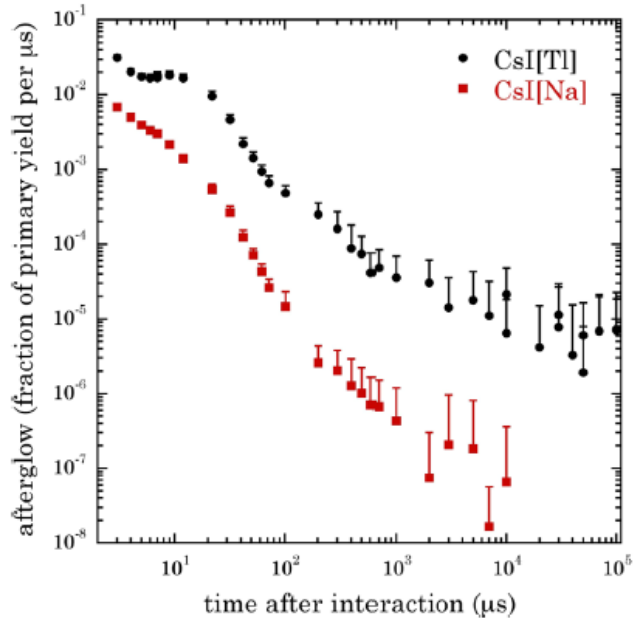


Fig. 3. Afterglow (phosphorescence) in CsI[Na] and CsI[Tl] scintillators. This figure shows the integrated PMT current detected over one  $\mu\text{s}$ , at times following gamma energy depositions of  $1.5 (\pm 0.2)$  MeV, as a fraction of the same for the initial primary scintillation. A combination of single-channel analyzer and a gate generator was used to trigger a waveform digitizer in this measurement. Only positive statistical error bars are shown for clarity. Each data point is the average of 100 measurements. Identical small crystals of each material were used, obtained from the same source [25] as the 2 kg and 14 kg CsI[Na] detectors discussed in the text. CsI[Tl] is notorious for its excessive afterglow. This limits its use in several applications [26], including a CENNS measurement in a site lacking significant overburden (see text).

- CsI[Tl] is notorious for its excessive afterglow
- CsI[Na] lacks the excessive afterglow
  - > Advantage for afterglow cut( $\sim 0.75$  signal acceptance fraction)

2015 R&D paper

# Experimental Setup: CE $\nu$ NS Detector

- Spallation Neutron Source(SNS) at Oak Ridge National Laboratory

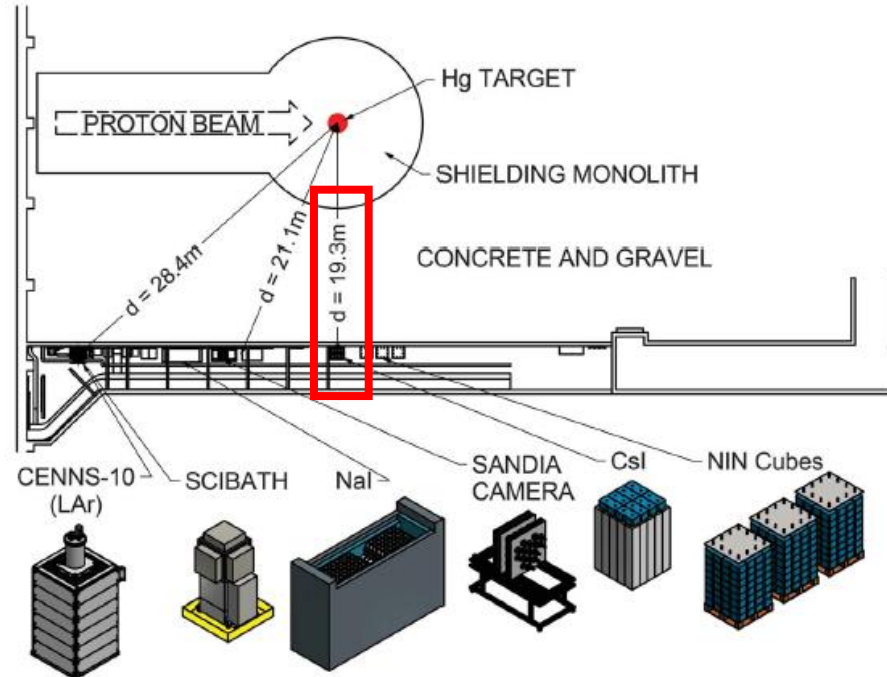
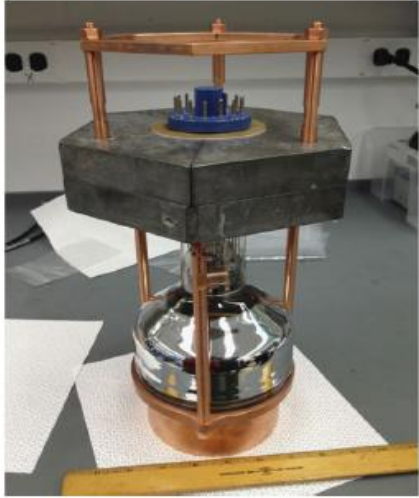


**Fig. 2. COHERENT detectors populating the “neutrino alley” at the SNS.** Locations in this basement corridor profit from more than 19 m of continuous shielding against beam-related neutrons and a modest 8 m.w.e. overburden able to reduce cosmic ray-induced backgrounds, while sustaining an instantaneous neutrino flux as high as  $1.7 \times 10^{11} \nu_{\mu} \text{ cm}^{-2} \text{ s}^{-1}$ .

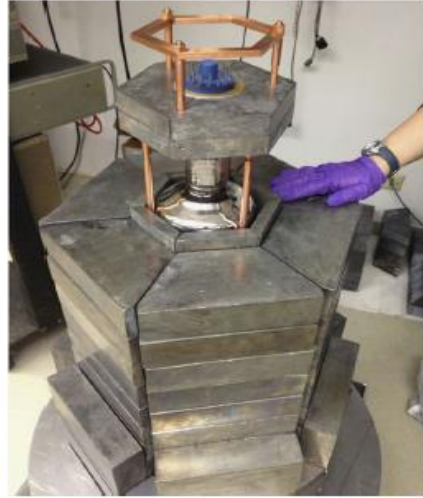
- CE $\nu$ NS Detector populating the “neutrino alley” at the SNS
- $10^{14}$  protons per 1 bunch (beam rate : 60 Hz, energy : 1 MW)
- Protons-on-target (POT, target : mercury) produce pions ( $0.08 \pi^+$  are produced per proton)
- Stopped  $\pi^+$  decay at rest with production of mono-energetic 30 MeV  $\nu_{\mu}$  : “prompt” neutrinos
- $\mu^+$  from pion decay travels tenth of a millimeter and decays at rest with production of  $\bar{\nu}_{\mu}$  and  $\nu_e$  : “delayed” neutrinos
- Neutrino flux at 20m from the SNS source:  $1.7 \times 10^7 \text{ cm}^{-2} \text{ s}^{-1}$

# Experimental Setup: CE $\nu$ NS Detector

- Shielding design



Crystal & PMT



lead



Muon veto panels

2015 prototype

2017 experiment

- 14.57 kg CsI[Na] crystal
- EJ-301 (Liquid scintillator) in water tank
- Around 15cm lead (low-activity 5cm lead)
- 15 cm high-density polyethylene (HDPE)
- 5cm muon veto around sides and top

# SNS neutrinos to the CsI[Na] detector(Geant4)

- Energy distribution and arrival time of SNS neutrinos to the CsI[Na] detector(Geant4)

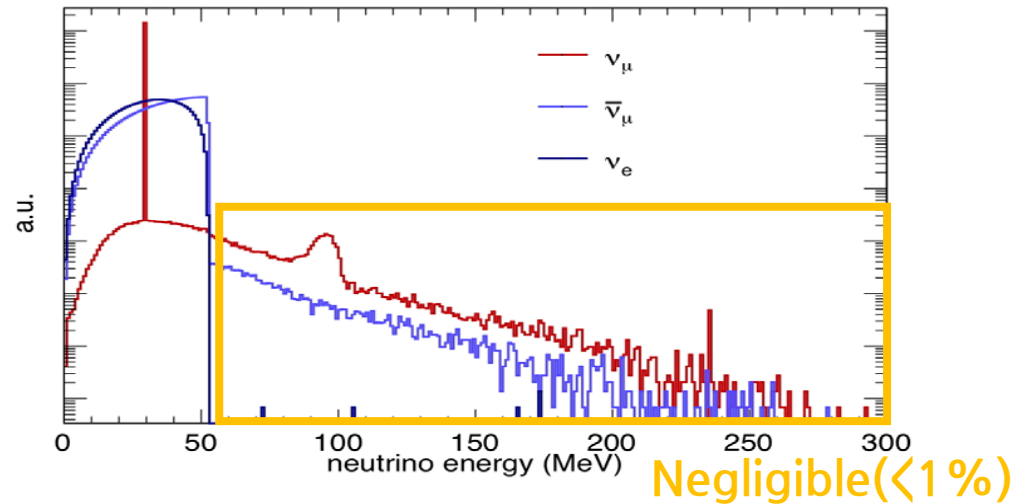
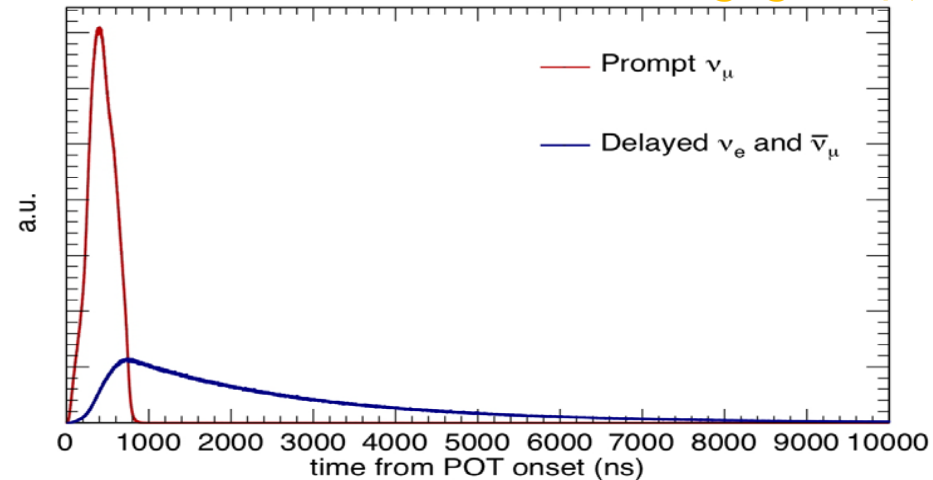


**Fig. S2.** Geant4 energy distribution and arrival time of SNS neutrinos to the CsI[Na] detector. Neutrinos above the endpoint of the Michel spectrum ( $\sim 53$  MeV) arise from DIF and muon capture, contributing a negligible ( $< 1\%$ ) signal rate. Delayed neutrinos follow the  $2.2 \mu\text{s}$  time constant characteristic of muon decay. A discussion on neutrino production rates (the normalization factors for these distributions) and associated uncertainties is provided in the supplementary materials text.



# Beam-related Background Studies

- Arrival time of neutron-like events in EJ-301 Scintillator(LS)

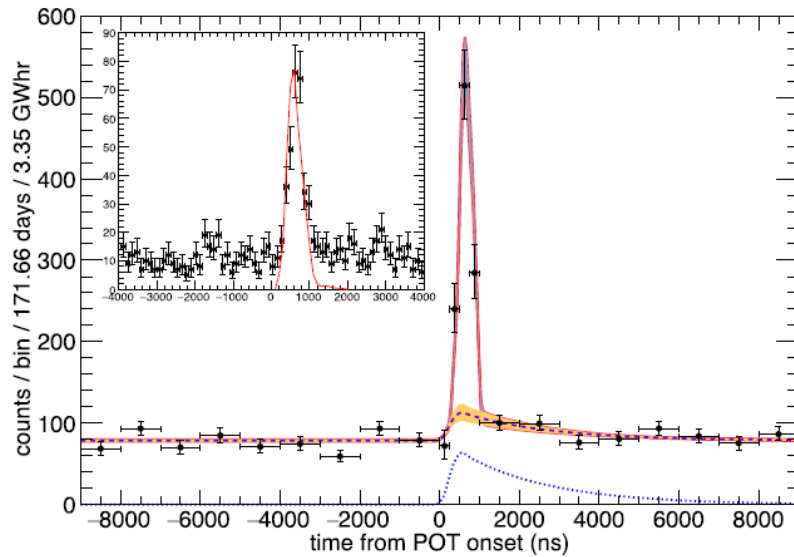
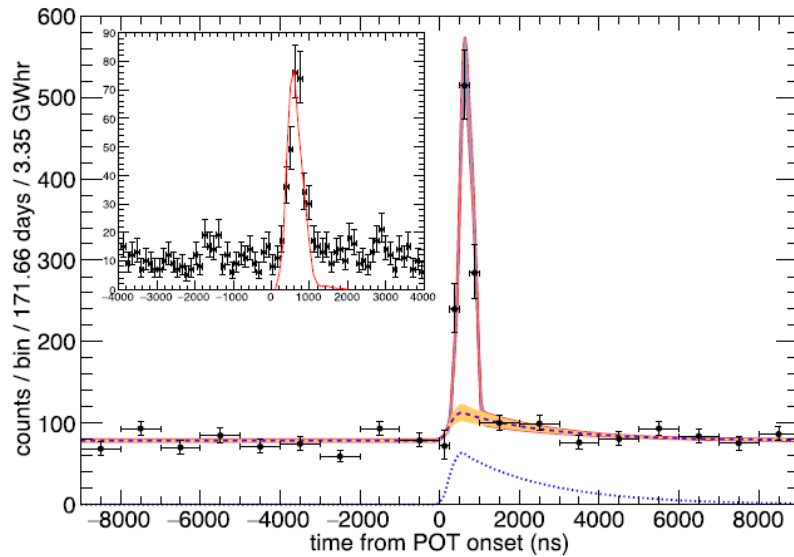


Fig. S3. Three-component unbinned fit to the arrival time of neutron-like events in EJ-301 scintillator cells (see text). Red lines delimit the one-sigma contour of the best-fit model. A dashed line indicates the best fit to NIN and environmental background components, a yellow band their one-sigma uncertainty. The presence of a non-zero NIN component is favored at the 2.9-sigma confidence level. However, the magnitude of this background is found to be negligible for a CEvNS search. A dotted line represents the predicted NIN component using the production rate calculated in (57,58). *Inset*: zoom-in using 100 ns bins. The red line is a normalized probability distribution function predicted by Geant4 for the arrival time of prompt neutrons contributing to the available 30-300 keV ionization energy region (Fig. S4). The simulation includes the time-profile of POT, provided by the SNS, and subsequent neutron production, moderation, and time-of-flight through 19.3 m of intermediate moderating materials (see text). This PDF is used to represent the prompt neutron component in our fits. The best-fit to its position agrees within errors ( $\pm 168$  ns) with the Geant4 prediction shown.

- Data structure
    - POT trigger position set :  $55 \mu\text{s}$
    - Pretraces: used to data cut removing events caused by afterglow from a previous energy deposition
    - Coincident:  $12 \mu\text{s}$  following POT triggers(signals)
    - Anti-Coincident:  $12 \mu\text{s}$  before POT triggers(to compare with Coincident)
-

# Beam-related Background Studies

- Arrival time of neutron-like events in EJ-301 Scintillator(LS)



**Fig. S3.** Three-component unbinned fit to the arrival time of neutron-like events in EJ-301 scintillator cells (see text). Red lines delimit the one-sigma contour of the best-fit model. A dashed line indicates the best fit to NIN and environmental background components, a yellow band their one-sigma uncertainty. The presence of a non-zero NIN component is favored at the 2.9-sigma confidence level. However, the magnitude of this background is found to be negligible for a CEvNS search. A dotted line represents the predicted NIN component using the production rate calculated in (57,58). *Inset:* zoom-in using 100 ns bins. The red line is a normalized probability distribution function predicted by Geant4 for the arrival time of prompt neutrons contributing to the available 30-300 keV ionization energy region (Fig. S4). The simulation includes the time-profile of POT, provided by the SNS, and subsequent neutron production, moderation, and time-of-flight through 19.3 m of intermediate moderating materials (see text). This PDF is used to represent the prompt neutron component in our fits. The best-fit to its position agrees within errors ( $\pm 168$  ns) with the Geant4 prediction shown.

- Dashed blue line indicates the best fit to NIN(neutrino-induced neutrons) and environmental background components
- Yellow band their one-sigma uncertainty
- The magnitude of this background is found to be negligible

# Beam-related Background Studies

- $^{252}\text{Cf}$  calibration data vs SNS data

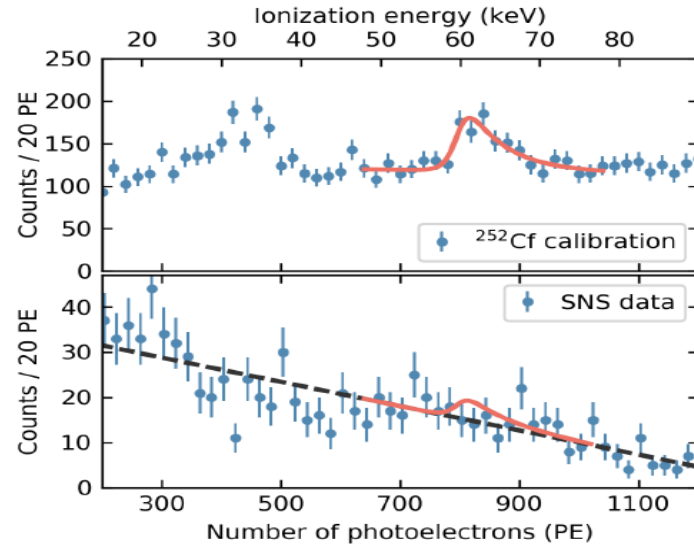
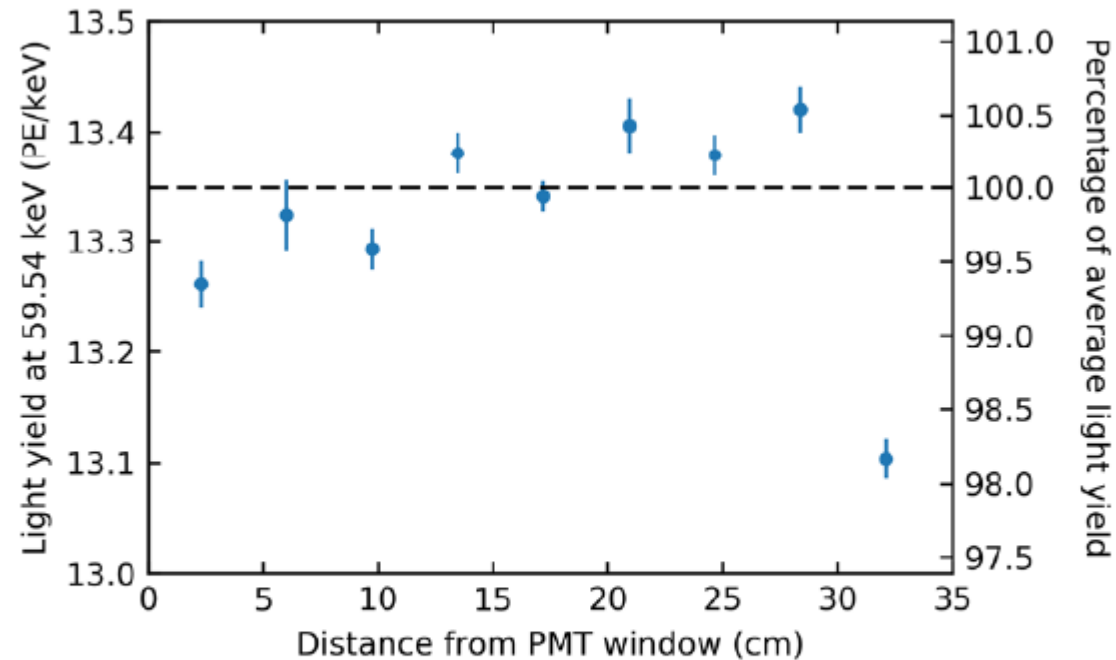


Fig. S5. *Top*: energy depositions in CsI[Na] during deployment of a  $^{252}\text{Cf}$  neutron source outside of the detector shielding, using self-triggering of the detector. A neutron inelastic scattering peak (57.6 keV) is visible at  $\sim 60$  keV, with a second from the electron capture decay of  $^{128}\text{I}$ , at 31.8 keV. The small shift to a higher energy and “shark tooth” shape for the inelastic peak arise from the addition of recoiling nucleus and gamma de-excitation energies (62). This peak is correctly predicted in shape and rate by an MCNPX-PoliMi simulation (see text). The red line represents a fit to this region, using an *ad hoc* peak template and flat background. *Bottom*: Energy depositions in CsI[Na] during the 200-1100 ns arrival interval associated with prompt neutron arrival (Fig. S3), for all Beam ON periods collected (308.1 live-days). The red line shows the 90% C.L. maximum number of counts allowed by a fit using the same peak template and fitting window, and a simple background model (dashed black line). The best-fit number of counts under this peak is  $3.9 \pm 11.1$ , compatible with zero. An additional bound on the magnitude of the prompt neutron background can be extracted from the absence of an obvious inelastic peak (see text).

- $^{252}\text{Cf}$  calibration data: neutron inelastic scattering peak(57.6 keV) is visible at  $\sim 60$  keV
- SNS data: energy distribution during 200-1100 ns arrival interval  $\rightarrow$  prompt neutron arrival
- The best-fit number of counts(below fit) is  $3.9 \pm 11.1$
- Additional bound on the magnitude of the prompt neutron background can be extracted

# Light yield of CsI[Na] crystals

- Light yield using Am-241 source(59.54 keV)



- Around 13 PE/keV

**Fig. S6.** Measurements of electron recoil light yield uniformity along the length of the CsI[Na] CEvNS detector (see text).

# Quenching factor

- CsI[Na] quenching factor

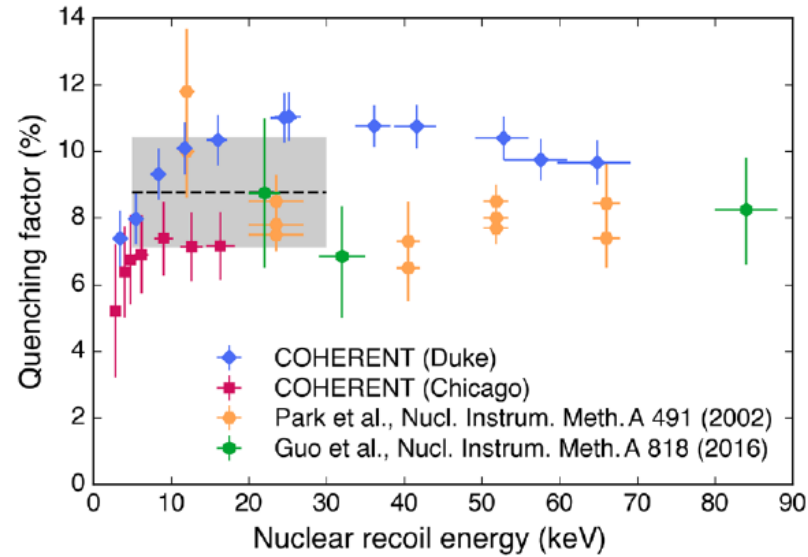


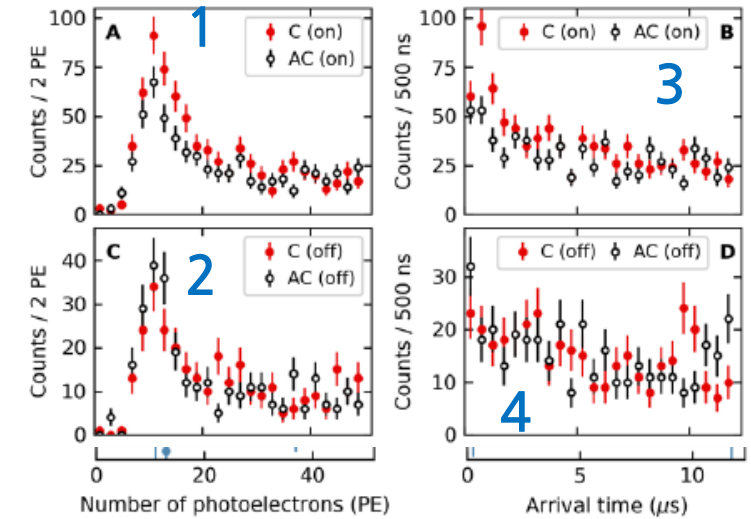
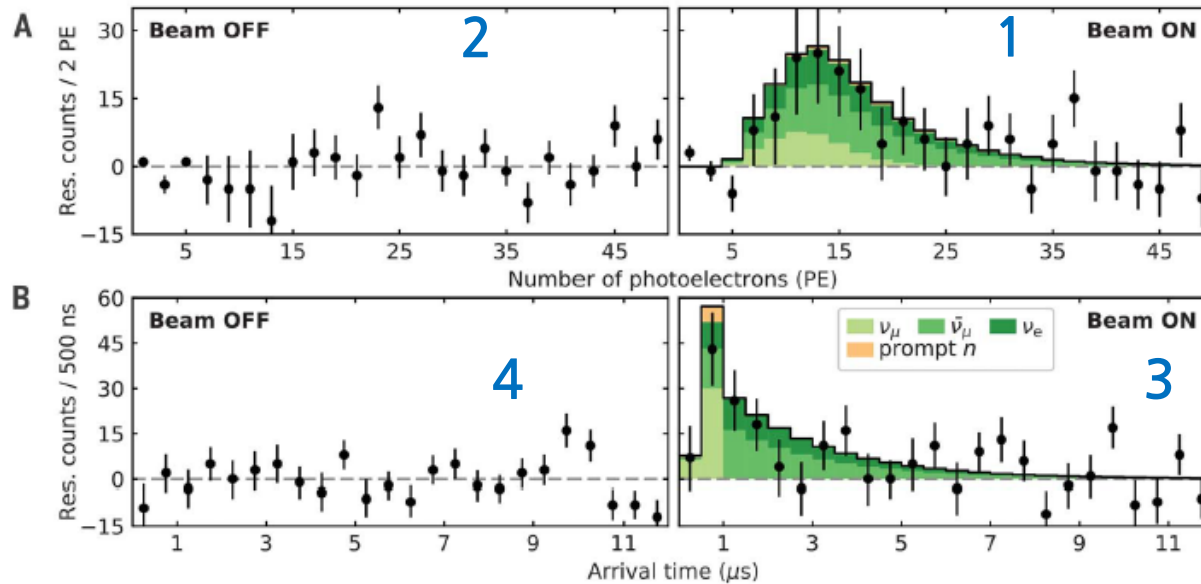
**Fig. S10.** Previous measurements of CsI[Na] quenching factor (67, 68), together with two new measurements performed within the COHERENT collaboration. These shared beam and target crystal, but differed in backing detectors, data acquisition, and approach to analysis. The grayed region spans the energy ROI for the present CEvNS search (~5-30 PE, Figs. 3 and S11). The reliability of semi-empirical QF models in this region being in question (69), we adopt the pragmatic approach of fitting all measurements in the ROI with a constant, weighting the experimental uncertainties shown in the plot (8.78 %, dashed line). Its uncertainty ( $\pm 1.66$  %, vertical grayed range) is conservatively derived from the unweighted standard deviation of all data points included in the fit. We find no evidence in our data for an enhanced nuclear/electron recoil discrimination in CsI[Na], as claimed in (68).

- Quenching factor : the ratio between the scintillation yields for electron recoils and nuclear recoils
- Using a monochromatic ( $3.8 \pm 0.2$  MeV) DD neutron beam at the Triangle Universities Nuclear Laboratory(TUNL)

# Result

- Observation of coherent elastic neutrino-nucleus scattering

**Fig. 3. Observation of coherent elastic neutrino-nucleus scattering.** (A and B) Residual differences (data points) between CsI[Na] signals in the 12  $\mu$ s after POT triggers and those in a 12- $\mu$ s window before, as a function of (A) their energy (number of photoelectrons detected) and (B) event arrival time (onset of scintillation). Steady-state environmental backgrounds contribute to both groups of signals equally, vanishing in the subtraction. Error bars denote SD. These residuals are shown for 153.5 live days of SNS inactivity ("Beam OFF") and 308.1 live days of neutrino production ("Beam ON"), over which 748 GWh of energy ( $\sim 1.76 \times 10^{23}$  protons) was delivered to the mercury target.



- (Coincident) - (Anti-coincident)
- > Residual counts

- Beam On days : 308.1 live days
- Beam Off days : 153.5 live days



- Observed at the  $1\sigma$  level :  $134 \pm 22$  events
- Consistency with standard model :  $173 \pm 48$  predicted

- 1.17 photoelectrons are expected per keV(nuclear recoil energy)

# Next plan

---

- 1-ton liquid argon(LAr) detector with nuclear/electron recoil discrimination capability
- 2-ton NaI[Tl] array simultaneously sensitive to sodium CE $\nu$ NS and charged-current interactions in iodine
- P-type point contact germanium detectors with sub-keV energy threshold

# Neutrino Elastic-scattering Observation with NaI(NEON)

---



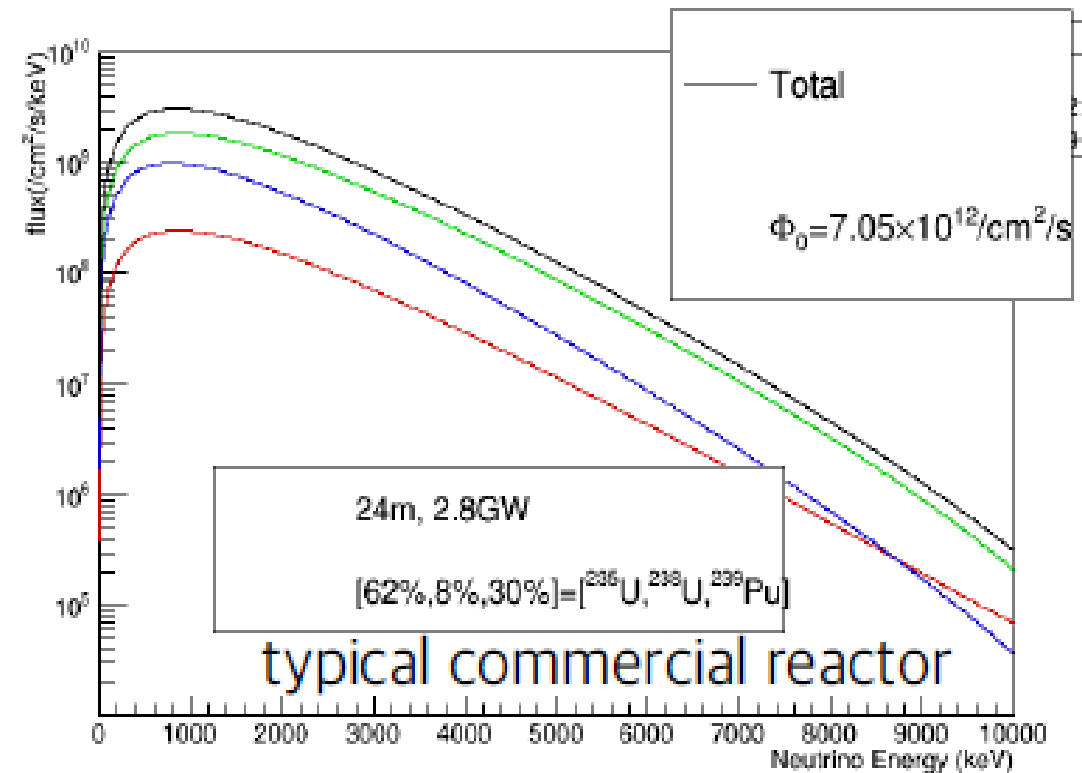
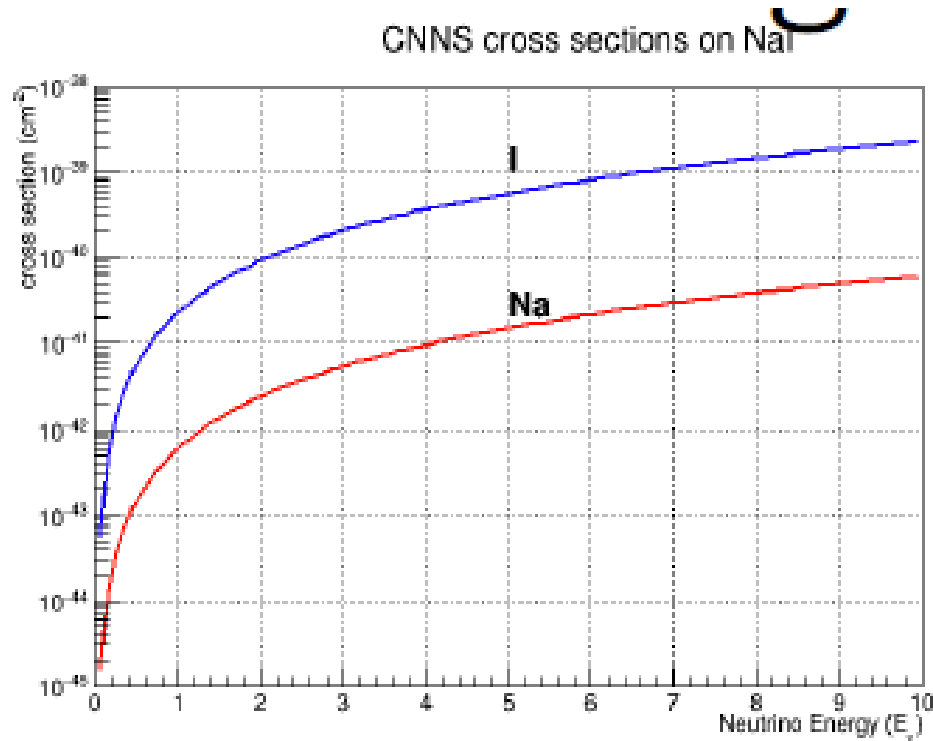
- Hanbit Nuclear Power Plant(Yonggwang)

# Motivation

---

- To detect coherent neutrino-nucleus scattering with NaI[Tl] detector from reactor
- To expand knowledge of neutrino properties (sterile neutrino, neutrino magnetic moment, nuclear structure and so on)
- Similar to COSINE experiment

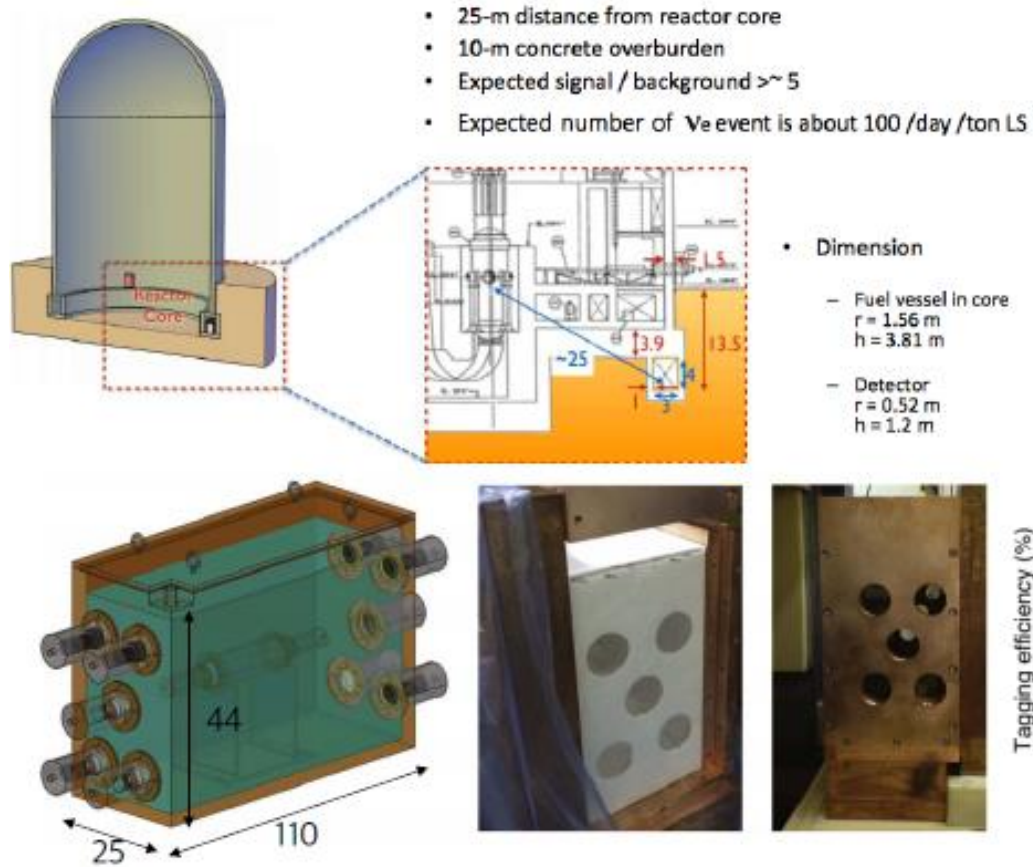
# Background(cross section, recoil energy spectrum)



- Cross section on NaI

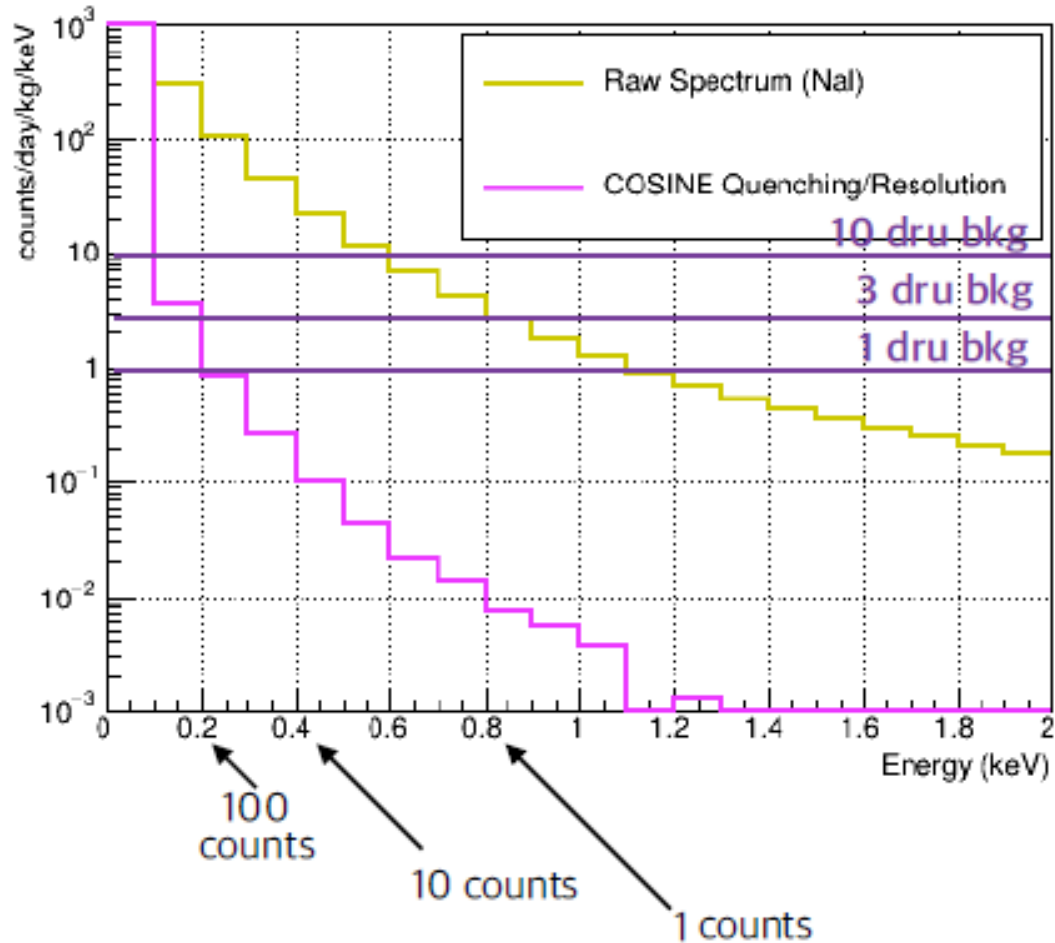
- Reactor neutrino recoil energy spectrum

# NEON Experiment



- A prototype copper box exists in HQ basement
- Around 10cm lead needed
- Around 30cm PE shields needed
- LS exists in HQ experiment room
- 4 × 2 kg crystals(2 R&D crystals, 2 delivery)

# NEON Experiment



- Assume 10 kg crystal, 100 day

- Assume COSINE measured quenching with C6 crystal background/event selection
- Low threshold is necessary
- High light yield of crystal is needed(R&D is ongoing)

# Challenges

- Neutrino-Iodine cross section is x30 larger than Neutrino-Sodium ( $N^2$  dependence)
- Iodine (127) is heavier than sodium (23)
  - Therefore, Iodine nuclei recoil less than sodium
  - E.g. 10 MeV nu max recoil energy is 7.4 keV on Na and 1.6 keV on I
- Also, increasing large amount of sodium is not trivial,
  - 10 kg NaI crystal contains 1.5 kg of sodium target.
- Light emission (quenching) is smaller in iodine than in sodium.

$$E_{rec}^{max} = 2E_{\nu}^2/M$$

Impossible to change

- Below 0.5 keV is achievable in NaI?
  - All PMT noise can be rejected?
- What is quenching in these energies?
- Can we lower the scintillation background?
- How would the downgoing muons affect?

Not impossible

# Status(HQ basement(C106))

---

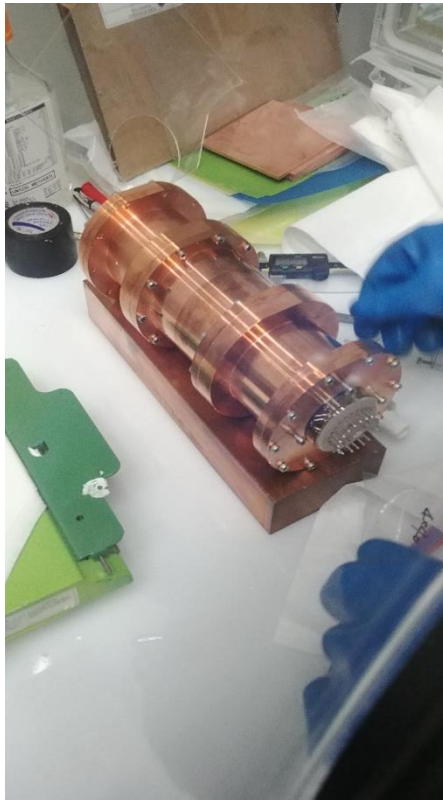


- DAQ system installed(similar to COSINE)

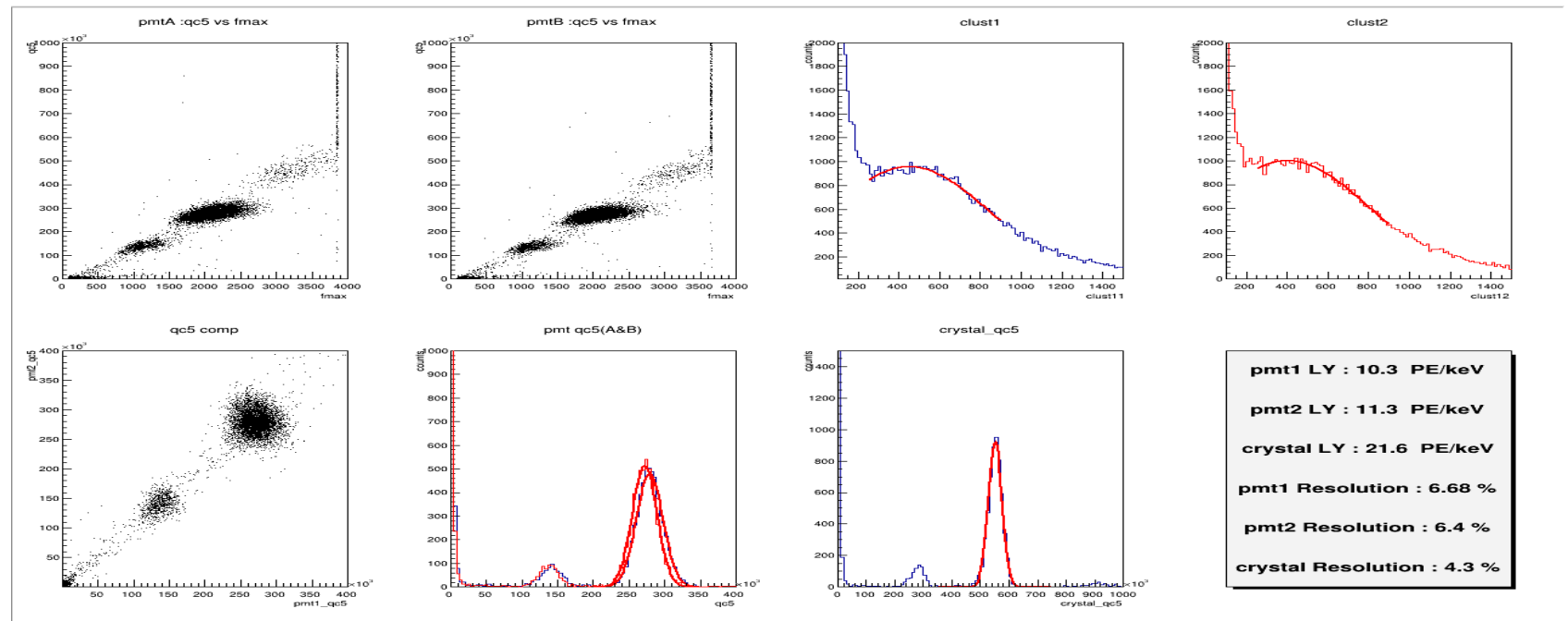
- Shielding prototype

# R&D crystal

- Goal of NaI[Tl] light yield is 30 PE/keV(to achieve low threshold)
- Polishing crystal to match pmt diameter(3 inch).



- NaI-032



- Light yield of 4-inch NaI-032 crystal : around 13 PE/keV
- Light yield of 8cm(>3-inch) NaI-032 crystal : around 21 PE/keV

# R&D crystal

---

## Improvement points

- Polishing crystal to match pmt diameter precisely(3 inch)
- Setting glove box less humidity and dehydrating other equipment when encapsulating NaI crystal
- Light yield could be increased at moderately low temperature

# Summary

---

- Succeeded in observing coherent elastic neutrino-nucleus scattering using CsI[Na] detector
- NEON experiment R&D is ongoing

# Backup